Concept of a Single Temperature for Highly Nonequilibrium Laser-Induced Hydrogen Desorption from a Ruthenium Surface

G. Füchsel,[1] J. C. Tremblay,[1] T. Klamroth,[1] P. Saalfrank,[1] and C. Frischkorn[2]
[1]*Institut für Chemie, Universität Potsdam, Karl-Liebknecht-Straße 24-25, D-14476 Potsdam-Golm, Germany*
[2]*Institut für Experimentalphysik, Freie Universität Berlin, Arnimallee 14, 14195 Berlin, Germany*
(Received 23 April 2012; published 30 August 2012)

Laser-induced condensed phase reactions are often interpreted as nonequilibrium phenomena that go beyond conventional thermodynamics. Here, we show by Langevin dynamics and for the example of femtosecond-laser desorption of hydrogen from a ruthenium surface that light adsorbates thermalize rapidly due to ultrafast energy redistribution after laser excitation. Despite the complex reaction mechanism involving hot electrons in the surface region, all desorption product properties are characterized by equilibrium distributions associated with a single, unique temperature. This represents an example of ultrahot chemistry on the subpicosecond time scale.

DOI: 10.1103/PhysRevLett.109.098303 PACS numbers: 82.60.−s, 05.70.Np, 79.20.La, 82.20.Wt

Classical thermodynamics provides a complete picture to predict the outcome of chemical processes under normal thermal conditions. With the advent of femtosecond laser chemistry, the question that arises is, can it still provide an accurate microscopic description of ultrafast, electron-driven reactions that are dynamically brought far from equilibrium? In most cases, experimental findings point to a much more complex mechanism involving transient species. In fact, nonequilibrium distributions have been shown to persist for photoexcited electrons in Ru(0001) for a few hundred femtoseconds (fs) before they thermalize [1]. It comes then as no surprise that nuclear degrees of freedom with their larger masses and weaker couplings are not expected to thermalize at all on a subpicosecond time scale during femtosecond laser experiments at surfaces, and experience with many systems supports this view [2,3]. Still, temperatures are often assigned to explain the energy content of molecular reaction products of hot electron-mediated femtosecond laser experiments. The nonequilibrium character of the reaction then manifests in the need of different temperatures for different degrees of freedom, e.g., translations, vibrations, and rotations. In this Letter, we provide arguments, however, that hot electron-mediated dynamics of light, mobile adsorbates at metallic surfaces can well be rationalized by a single, effective temperature, implying ultrafast thermalization also for nuclear degrees of freedom. This will be exemplified by the femtosecond laser-induced recombinative desorption (FLD) of hydrogen from ruthenium,

$$2\mathrm{H}_{\mathrm{ads}}/\mathrm{Ru}(0001) \rightarrow \mathrm{H}_2 + \mathrm{Ru}(0001),$$

that was previously studied experimentally in Refs. [4–6].

Using 130 fs-laser pulses in the fluence range of 50–120 J/m^2, the desorption reaction shows large isotope effects: upon deuteration, the desorption yields Y and the translational energies decrease significantly. It was observed that the yield increases nonlinearly with the laser fluence according to the power law $Y \propto F^n$, where n is approximately 3. Also, the translational energy of the desorbed species is found to be much larger than the internal, vibrational, and rotational energies, pointing toward an overall nonthermal nature for the reaction.

In recent theoretical work [7], full dimensional molecular dynamics simulations with electronic friction (MDEF) [8], called MDEF(T_{el}) in the following, were performed using a classical Langevin formalism, where

$$m\frac{d^2\underline{r}_i}{dt^2} = -\frac{\partial V(\underline{r}_1,\underline{r}_2)}{\partial \underline{r}_i} - \eta(\underline{r}_i)\frac{d\underline{r}_i}{dt} + \underline{\mathcal{R}}_i(t) \qquad (1)$$

were solved as equations of motion for two mobile hydrogen atoms ($i = 1, 2$) on Ru(0001): H(1 × 1). The potential function $V(\underline{r}_1, \underline{r}_2)$ and atomic friction coefficient $\eta(\underline{r}_i)$ were determined from periodic density functional theory. Random forces $\underline{\mathcal{R}}_i(t)$ are Gaussian white noise depending on the electronic temperature $T_{\mathrm{el}}(t)$.

We used a two-temperature model (2TM) [9] to calculate the time profile of the substrate electronic temperature $T_{\mathrm{el}}(t)$ caused by the response of the surface electrons to a fs-laser field of fluence F. As shown in the left panel of Fig. 1, $T_{\mathrm{el}}(t)$ (green line) rises up to several 1000 K within ∼500 fs and equilibrates with the phonons [$T_{\mathrm{ph}}(t)$, red line] after ∼1500 fs. Hot electrons in the surface couple simultaneously with the adsorbate, heating up its degrees of freedom and leading to desorption at a rate $R(t)$, predominantly during the first 2 ps after laser excitation. Using the 2TM seems a contradiction to Ref. [1], but in fact most desorption events take place when $T_{\mathrm{el}}(t)$ is around its maximum, where the 2TM was found to be valid. Indeed, all experimental reaction features could be well rationalized by a purely hot electron-mediated Langevin model. This also indicated that the reaction is mostly determined by the topology of the ground state potential. Similar results were obtained by Luntz *et al.* [10] for reduced-dimension classical Langevin simulations, which

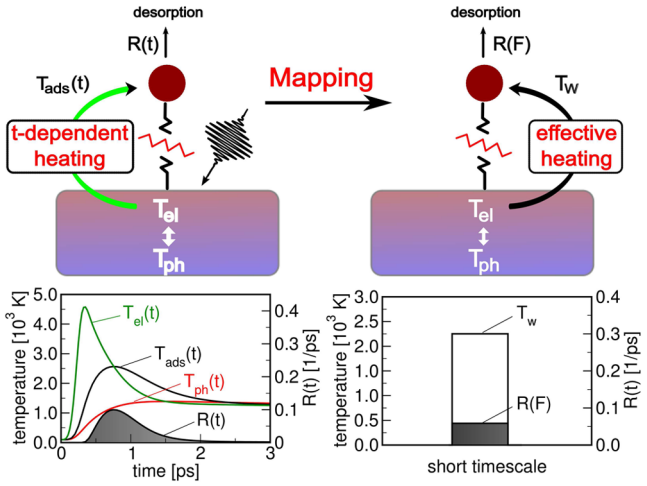

FIG. 1 (color online). Desorption of D_2 from Ru after excitation with a 130 fs Gaussian laser pulse at 800 nm, $F = 140$ J/m^2. Left panel: time-dependent behavior of the electron, phonon, and adsorbate temperatures from a 2TM or 3TM, and the desorption rate from the 3TM according to Eq. (2). Right panel: the hot electron-mediated dynamics is mapped to an effective heating mechanism.

also showed that phonons play only a marginal role in the FLD.

A frequently used alternative that bypasses costly MDEF calculations is provided by a kinetic model extending the 2TM to a three-temperature model (3TM). Admitting a barrier of height E_a for desorption, $R(t)$ can then be computed by [7,11,12]:

$$R(t) = \frac{\Gamma E_a}{k_B T_{\mathrm{ads}}(t)} \exp\left(-\frac{E_a}{k_B T_{\mathrm{ads}}(t)}\right). \tag{2}$$

The potential used here predicts a binding energy of 856 meV and a classical adsorption barrier of $E_0 = 186$ meV, yielding a desorption barrier of $E_a = 1042$ meV [7,13]. For a purely electron-driven reaction, the adsorbate temperature [$T_{\mathrm{ads}}(t)$, black line in Fig. 1] can be calculated from

$$\frac{dT_{\mathrm{ads}}(t)}{dt} = \Gamma[T_{\mathrm{el}}(t) - T_{\mathrm{ads}}(t)]. \tag{3}$$

The effective energy transfer rate Γ is closely related to the electronic friction coeffcient η shown above. It was chosen as $\Gamma = (210\ \mathrm{fs})^{-1}$ and $(420\ \mathrm{fs})^{-1}$ for H_2 and D_2, respectively [7]. The factor of 2 reflects the mass ratio between H_2 and D_2, making the vibration-electron hole pair coupling more efficient for the lighter isotope [14]. Eqs. (2) and (3) represent a simple tool producing similarly accurate results as the MDEF(T_{el}) methodology. As an example, the rate profile $R(t)$ from 3TM is shown as a shadowed curve in Fig. 1, and found to agree well with the MDEF(T_{el}) result (see Ref. [7]).

We proceed to show that the process can be well rationalized with an even simpler model, by mapping the fluence F to an effective temperature T_w that captures all the physics of the adsorbate excitation. Following Ref. [6], T_w is obtained by integrating the time-dependence of Eqs. (2) and (3),

$$F \leftrightarrow T_w = \frac{\int_0^\infty T_{\mathrm{ads}}(t) R(t) dt}{\int_0^\infty R(t) dt}. \tag{4}$$

In this picture, surface excitation leads to an instantaneous effective heating of the adsorbate degrees of freedom, which in turn can be characterized by equilibrium energy distributions at the same constant temperature T_w. As shown in the right panel of Fig. 1, the reaction rate and the effective temperature must remain constant over a short period of time (femtoseconds) to mimic the ultrashort character of the process. T_w fully determines the microscopic properties of the desorbed molecules.

The values of T_w corresponding to a purely electron-driven reaction are listed in Table I for H_2 and D_2 as a function of F. We obtained effective adsorbate temperatures between about 1300 and 3000 K. The values for D_2 are lower than those for H_2 at the given laser fluence because of the smaller effective energy transfer, characterized by Γ. This fact emphasizes the influence of Γ on the value of T_w, whereas E_a does not have significant impact due to the averaging procedure Eq. (4).

To validate our model, we first compare previous MDEF(T_{el}) simulations with the experimental results of Refs. [5,6]. As seen from Fig. 2(a), the translational energies of desorbed H_2 and D_2 as a function of F are well reproduced by theory. In Fig. 2(b), the same MDEF(T_{el}) results are mapped to the effective temperature picture according to Eq. (4). Also shown are MDEF translational energies obtained from the trajectories at constant temperatures chosen in the same range of T_w as for the MDEF(T_{el}) simulations (the red triangles and squares "model"). The following conclusions can be drawn. (1) The results are independent, whether one uses a constant effective temperature or the "true" time-dependent electronic temperature to simulate the FLD. In both cases,

TABLE I. Effective adsorbate temperatures T_w (in K) obtained from Eqs. (2)–(4). Parameters: $E_a = 1.042$ eV, $\Gamma_{\mathrm{H}} = (210\ \mathrm{fs})^{-1}$, and $\Gamma_{\mathrm{D}} = (420\ \mathrm{fs})^{-1}$. $T_{\mathrm{el}}(t)$ was calculated from the 2TM for 130 fs Gaussian laser pulses.

F [J/m^2]	60	80	100	120	140	160
$T_w(H_2)$	1746	2074	2360	2611	2832	3029
$T_w(D_2)$	1332	1606	1850	2073	2277	2469

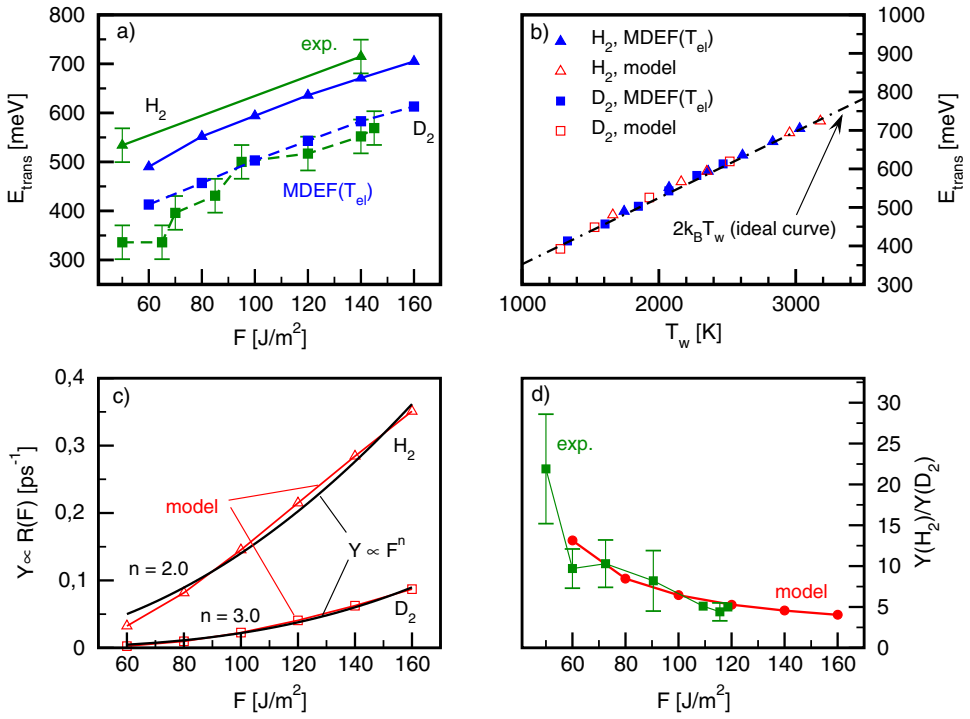

FIG. 2 (color online). (a) Comparison of 6D MDEF(T_{el}) translational energies (blue, dark gray) to experimental results (green, light grey) for different fluences. (b) Comparison of the effective temperature model (open red squares and triangles) and MDEF(T_{el}) simulations (solid blue squares and triangles) as a function of T_w. The ideal thermal behavior $E_{trans} = E_0 + 2k_BT_w$ is also shown (dashed line, $E_0 = 180$ meV). (c) The dependence of the reaction yield on F obtained from our temperature model (red, symbols) and a nonlinear fit $Y \propto F^n$ (solid black lines) is shown for H_2 and D_2. (d) Isotope ratios are compared to experiment [5].

the translational energy increases linearly with the temperature T_w and exhibits an ideal thermal behavior; i.e., E_{trans} grows with a slope of $2k_B$ with T_w, as expected for a thermal ensemble of molecules translating in a 3D half-space above the surface [2]. The internal, rovibrational energy (not shown) increases slightly more rapidly with the effective temperature ($E_{int} = 2.2k_BT_w$) than the ideal value for a molecule with two rotations and one vibration (also $2k_BT_w$), again for both models. This is due to the coupling of the translational and internal degrees of freedom close to the transition state. (2) Astonishingly, all isotopic effects vanish in the temperature picture. The observed experimental difference results from different effective adsorbate temperatures T_w for the two isotopes and, hence, from different energy transfer rates Γ. (3) In the limit $T_w \to 0$ K, a linear regression yields an adsorption barrier of $E_0 = 180$ meV close to the experimental value of 215 meV [6]. This causes higher translational than internal energies, i.e., $E_{trans} = E_0 + 2k_BT_w$ and $E_{int} = 2k_BT_w$, in agreement with experiment. Nonetheless, the desorbed molecules are well characterized by a single temperature T_w.

The effective temperature model provides a very intuitive understanding and a quantitative description of the intricate coupled electron-nuclear dynamics at work during the FLD. We can use T_w from Table I to calculate the isotopic ratios $Y(H_2)/Y(D_2)$ and the nonlinear increase of the desorption yield with the laser fluence. In the following, we consider a photodesorption process with a constant reaction rate $R(F)$ induced by a laser of fluence F. On short time scales, the desorption yield remains small, which allows us to set Y proportional to $R(F)$ in the quasistationary approximation

$$Y \propto R(F) = \frac{\Gamma E_a}{k_B T_w(F)} \exp\left(-\frac{E_a}{k_B T_w(F)}\right). \qquad (5)$$

In Fig. 2(c), the rate $R(F)$ is plotted against F, where a nonlinear fit $Y \propto F^n$ gives $n = 2.0$ for H_2 and $n = 3.0$ for D_2. These values compare reasonably well with the experiment ($n = 2.8$ and $n = 3.2$, respectively).

Further, the isotopic ratio can be obtained by calculating the ratio of the rates obtained from Eq. (5) for both isotopes at the given T_w. The theoretical predictions are compared to the experimental result in Fig. 2(d), in the range $F \in [60, 160]$ J/m^2. We find excellent quantitative agreement with the experiment. At low fluences, small discrepancies arise from experimental uncertainties that are larger than the statistical error bars shown in the figure due to low desorption intensities [5].

To clarify if the thermal features of the MDEF simulations stem from the underlying classical description of the

process, we investigated the laser-induced desorption quantum mechanically beyond the single-potential energy surface model. In the energy regime investigated here, nuclear spin coupling is expected to play only a minor role, and consequently neglected. Laser heating promotes the adsorbate from the ground to an excited electronic state, driving the dynamics away from equilibrium. Quantum dynamical desorption induced by electronic transition (DIET) simulations were carried out using Gadzuk's surface hopping scheme [15] to roughly model the FLD at a low fluence. Here, F falls in the range $[50, 85]$ J/m^2, comparable to the experiment. A two-state model (TS model) consisting of the electronic ground and an effective electronic excited state associated with a lifetime τ_{el} is used to drive the dynamics. In the DIET regime, desorption results from a single electronic excitation–deexcitation cycle. The excited state is approximated by a shifted ground state potential raised by an energy ΔV [16,17]

$$V_e = V_g(X, Y, Z + \Delta Z, r - \Delta r, \theta, \phi) + \Delta V. \quad (6)$$

Here, $\{X, Y, Z\}$ are center-of-mass coordinates and $\{r, \theta, \phi\}$ describe the interatomic distance of the nascent hydrogen molecule and the orientation relative to the surface. The shift parameters Δr and ΔZ correspond to an Antoniewicz model [16,18], which accounts for the electrostatic attraction between an ion resonance and its image charge. To provide a good microscopic description of the energy redistribution upon excitation, the r- and Z-modes, and the rotational motion along ϕ are included in the dynamics. All other coordinates are fixed at their values at the adsorption minimum, which reduces the computational burden.

Similar conclusions regarding the properties of the desorbed molecules hold true for the quantum mechanical treatment. Fig. 3 shows the population of the rotational states of desorbed D_2 for different vibrational quantum numbers $\nu = 0$, 1, 2, obtained from 3D DIET-Antoniewicz simulations with $\tau_{el} = 2$ fs. The population

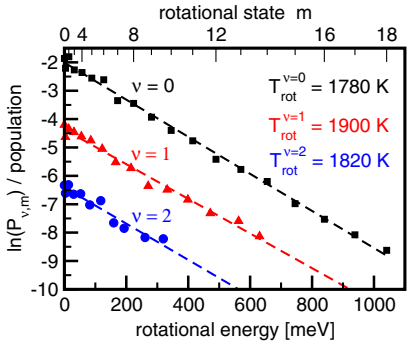

FIG. 3 (color online). Quantum mechanical DIET-Antoniewicz simulations for D_2 in 3D. Shown is the population of rotational states m for the vibrational states $\nu = 0$ (black squares), $\nu = 1$ (red triangles), and $\nu = 2$ (blue dots). Boltzmann fits are depicted by dashed lines.

distribution exhibits a Boltzmann behavior with an average temperature of $T_{rot} = 1830$ K, more or less independently of the vibrational states. Likewise, we obtain a rotational temperature of $T_{rot} = 2320$ K for H_2. These temperatures correspond to quantum mechanical energies of 89 meV for H_2 and 67 meV for D_2, which are close to the measured value of 80 meV for the latter at $F = 85$ J/m^2 [6]. From a Boltzmann plot, we obtain similar vibrational temperatures of $T_{vib} = 2500$ K for H_2 and $T_{vib} = 1850$ K for D_2. However, the experimental results show a more complex thermal behavior. The population of rovibrational states could only be fitted by using two distinct temperatures for two different rotational energy regimes. This may be attributed to collisional or dissipative deactivation, or to multiple electronic excitation effects, which are neglected here.

We also analyzed the translational energy distribution of the desorbing molecules. Shifting the origin to take into account the presence of the adsorption barrier E_0, the results are fitted to a one-dimensional Boltzmann distribution with a temperature T_{trans} according to [2]

$$\bar{P}(E_{trans}) = \left(\frac{1}{k_B T_{trans}}\right) \exp\left(-\frac{E_{trans} - E_0}{k_B T_{trans}}\right). \quad (7)$$

The barrier of $E_0 = 163$ meV is in good agreement with the classical result (180 meV, see above) and with the experimental prediction of 215 meV [6]. The profile of the simulated distribution is very well reproduced by Eq. (7) when using a temperature $T_{trans} = (\langle E_{trans} \rangle - E_0)/k_B = 1800$ K for D_2 and 2200 K for H_2. These results show that the rotational and vibrational temperatures discussed above are consistent with the translational temperatures, independently of the isotope. As was the case for the classical dynamics, each isotope is characterized by a single temperature for all its degrees of freedom, which is about 1800 K for D_2 and 2300 K for H_2.

At this point, we recall the experimental results for D_2 of Ref. [6], where a large difference between the translational and vibrational temperatures ($T_{trans} = 2500$ K and $T_{vib} = 1200$ K) was determined. Again, when taking the adsorption barrier of $E_0 = 215$ meV into account, both temperatures reach the same value of about 1200 K. The large differences between temperatures of different degrees of freedom discussed in Ref. [6] vanishes, which supports our claim that a single temperature suffices to characterize the desorbing molecules. It should not come as a surprise that the value of the single temperature differs from the quantum mechanical one. Indeed, the reduced-dimension treatment will inevitably lead to larger temperatures when considering molecules with the same energy in the exit channel.

In this Letter, we have reported on the theoretical treatment of the FLD of H_2 and D_2 from Ru(0001) induced by femtosecond laser fields. We showed that the translational, vibrational, and rotational energy distributions of the

desorbed molecules are very well reproduced by classical equilibrium thermodynamics using a single temperature. Nonadiabatic effects are expected to play a dominant role in the dynamics of light adsorbates at metallic surfaces. This leads to rapid thermal equilibration between the different types of motion due to very fast intramolecular vibrational energy redistribution, at least for such light adsorbates like hydrogen.

Our MDEF simulations show that the properties of the desorbing molecules can be reproduced quantitatively by using either a time-dependent electronic temperature approach or an effective, yield-weighted adsorbate temperature model. This again emphasizes the universal character of the single temperature model for describing the femtosecond dynamics of light adsorbates at metallic surfaces. Further, the effective temperature model is a very intuitive tool to understand the nature of the isotopic effects, originating from a species-dependent adsorbate-surface coupling constant Γ. Although a single temperature describes the energy distribution for each degree of freedom, quantization effects lead to an uneven energy partitioning, as was the case in the experiment [6]. On the other hand, the uneven temperature partitioning that was suggested to rationalize those findings was due to the classical treatment of the temperature-energy relation for the internal degrees of freedom. This does not hold for light molecules. Moreover, the activation barrier was not recognized as such. We therefore advocate using both temperatures and energies to characterize desorbing molecules in an FLD experiment on similar systems.

This work was funded by the Deutsche Forschungsgemeinschaft through Sonderforschungsbereich 450 and through project Sa 547/8-1.

[1] M. Lisowski, P. A. Loukakos, U. Bovensiepen, J. Stähler, C. Gahl, and M. Wolf, Appl. Phys. A **78**, 165 (2004).
[2] F. Zimmermann and W. Ho, Surf. Sci. Rep. **22**, 127 (1995).
[3] C. Frischkorn, J. Phys. Condens. Matter **20**, 313002 (2008).
[4] D. N. Denzler, C. Frischkorn, C. Hess, M. Wolf, and G. Ertl, Phys. Rev. Lett. **91**, 226102 (2003).
[5] D. N. Denzler, C. Frischkorn, M. Wolf, and G. Ertl, J. Phys. Chem. B **108**, 14503 (2004).
[6] S. Wagner, C. Frischkorn, M. Wolf, M. Rutkowski, H. Zacharias, and A. C. Luntz, Phys. Rev. B **72**, 205404 (2005).
[7] G. Füchsel, T. Klamroth, S. Monturet, and P. Saalfrank, Phys. Chem. Chem. Phys. **13**, 8659 (2011).
[8] M. Head-Gordon and J. C. Tully, J. Chem. Phys. **103**, 10137 (1995).
[9] S. I. Anisimov, B. Kapeliovich, and T. Perelman, Sov. Phys. JETP **39**, 375 (1974).
[10] A. C. Luntz, M. Persson, S. Wagner, C. Frischkorn, and M. Wolf, J. Chem. Phys. **124**, 244702 (2006).
[11] M. Brandbyge, P. Hedegard, T. F. Heinz, J. A. Misewich, and D. M. Newns, Phys. Rev. B **52**, 6042 (1995).
[12] D. M. Newns, T. F. Heinz, and J. A. Misewich, Prog. Theor. Phys. Suppl. **106**, 411 (1991).
[13] M. Luppi, R. A. Olsen, and E. J. Baerends, Phys. Chem. Chem. Phys. **8**, 688 (2006).
[14] M. Head-Gordon and J. C. Tully, J. Chem. Phys. **96**, 3939 (1992).
[15] J. W. Gadzuk, L. J. Richter, S. A. Buntin, D. S. King, and R. R. Cavanagh, Surf. Sci. **235**, 317 (1990).
[16] G. Füchsel, T. Klamroth, J. C. Tremblay, and P. Saalfrank, Phys. Chem. Chem. Phys. **12**, 14082 (2010).
[17] T. Vazhappilly, T. Klamroth, P. Saalfrank, and R. Hernandez, J. Phys. Chem. C **113**, 7790 (2009).
[18] P. R. Antoniewicz, Phys. Rev. B **21**, 3811 (1980).